

# Asset swap spreads as business cycle assessors : a Markov Switching Dynamic Factor with time-varying variance extension

Romain Aumond<sup>1</sup>

<sup>1</sup> ENSAE, Institut Polytechnique de Paris

## Abstract

This paper gauges the benefits of adding asset swap spreads in a real-time fashion to mitigate the usual caveats of asynchronous and lagging macroeconomic information in nowcasting models. This work sheds light on the capability of this weekly information to correctly assess the business cycle phases. We build upon the existing literature of Markov-Switching dynamic factor models a dynamic variance extension in the factor auto-regressive behavior. We show the advantage of the weekly market information flow, especially when applied to macro-based allocation strategies. The analysis is carried out on the United States. Asset swap spreads used as market sentiment proxy of current macroeconomic conditions improve the turning point detection process but also the risk/return couple of the implemented allocation strategies whenever a real-time macro dataset is used.

*Keywords:* Nowcasting; Bayesian Estimation; Dynamic Factor; Non-linearity

*JEL codes:* C11, C32, E27, E32, G11

---

\***Romain Aumond** Department of Economics, CREST-ENSAE. [romain.aumond@ensae.fr](mailto:romain.aumond@ensae.fr)

# 1. Introduction

Real time gauge of the state of the business economy has become an overarching question in the past decade for policy makers and market participants. In the wake of the Great Financial Crisis and the more recent Covid Pandemic, the heterogeneity of the contractionary episodes in terms of duration and amplitude has triggered hurdles for practitioners to properly identify the turning points of main street economy in a timely fashion. This work intends to show the credit market asset swap spreads capability to accurately track the economic downturn risks and occurrences. Those spreads are interpreted as a compensation of the Asset Swap (ASW) buyer for taking the credit risks (O’Kane (2000)). Another major advantage of this information sample is the daily availability of the market prices which in turn, enables to bypass the caveats related to the nowcasting literature; namely the asynchronicity in the publication of lagged economic data. The paper’s bedrock is to consider the default pricing capacity of the credit market as a relevant real-time predictor of the real economy booms and busts. We thus rely on the market efficiency hypothesis through the financial accelerator mechanism : a negative shock to business economy triggers an immediate alteration in corporate balance sheets and a decline in expected revenues. This deterioration further hampers investment capabilities and finally output. This development is embodied in the widening of the spreads : among the rate buckets of corporate asset swaps, a broad -sometimes distorted- repricing of default probabilities occurs. If this specific tension in the credit market arise the spreads between high grade and poor grade swap contracts can directly have an influence on the turning point detection process. We therefore develop a market-based real-time indicator of US activity which follows the developments along the business cycle phases and captures the asymmetry and heterogeneity of the contractionary episodes. These market prices bring additional information to the usual macroeconomic datasets composed of lagged hard data.

One can observe a non-linear pattern in the co-movement of risks re-pricing through securities spreads grade buckets. We embed this non-linear behavior into a econometric framework allowing for regime switch in the dynamics of an unobserved factor, in the now popular class of Markov Switching Dynamic Factor models (MS-DFMs). This class of models in the nowcasting literature achieve to unify two properties of the business cycle dynamics observed by Burns and Mitchell (1946) : a co-movement diffused across several economic aggregates and asymmetries along the regime phases. These properties are also displayed in the ASW markets. MS-DFMs are based on the seminal work of Diebold and Rudebusch (1996) that bridged works of Stock and Watson (1991) who developed a linear coincident indicator summarizing the co-movement of several aggregate time series and Hamilton (1989) in identifying regimes in a given time-series model through a Markov-Chain specification. Kim and Yoo (1995) further expanded the specification in a multivariate case and alternate specifications were used by Chauvet (1998) and Kim and Nelson (1998). We add to the existing literature of MS-DFMs a specification including a time-varying variance in the common factor dynamic which follows a autoregressive conditional heteroskedastic (ARCH) or a generalized autoregressive conditional heteroskedastic (GARCH) process. It aims at taking into account a broader heterogeneity in the amplitude of the shocks affecting the cycle. This works is thus related to the recent developments of treating time-varying volatility in dynamic factor models in order to overcome the Covid shock in the data. One can mention the works of Marcellino et al.

(2016) and [Antolin-Diaz et al. \(2023\)](#). This econometric framework allows us to track the business cycle and to infer in a timely fashion the occurrence of the adverse shocks.

This paper builds upon a vast strand of literature using asset prices variations as real economic activity predictors<sup>1</sup>. Nonetheless it differs from the above cited literature in its objective : we are not interested into projecting economic dynamics to a short or medium term horizon ([Gilchrist et al. \(2009\)](#), [De Santis \(2016\)](#)). The exercise rather undertakes an assessment on a high frequency basis of the current economic conditions as being "filtered" by the credit markets. This is more in line with [Chauvet and Senyuz \(2016\)](#) who use the information content of US Bond market to produce an assessment of real economy downturns. The interactions between the credit market sentiment and the real economy and the leading relationship between the both ([López-Salido et al. \(2016\)](#)) is however out of scope. A considerable literature depicts the fact that spreads do not only reflect a contemporaneous state of the economy but also a hedge against adverse economic scenario ([De Santis \(2016\)](#)). A complementary work by [De Santis \(2018\)](#) also provides a measure of excess bond premia and fragmentation for the Euro Zone. This work refers to the co-movement across a broad range of asset swap spreads as a coherent real-time macroeconomic risk repricing. This broad repricing occurs when the expected contractionary macroeconomic episode becomes the core preoccupation of market participants. The co-movement also falls into [Burns and Mitchell \(1946\)](#) definition of pervasiveness characterizing the business cycle : nations organizing their work mainly in business enterprises face expansions in many economic activities but also recessions. We capture the cross-sector co-movement by the exhaustive coverage of asset swap spreads synthetic indices we use from sectors depicted in [Appendix A](#).

We show in this paper the ability of the credit market to gauge the business economy turning-point in real-time, thus bringing a extremely valuable information to practitioners. The identification of a contractionary episode tends to be reactive and enables to bypass the traditional caveat related of asynchronous lagged macroeconomic hard data. This work intends to compare textbook real-time turning point nowcasters as the ones introduced by [Chauvet \(1998\)](#) and the new specification proposed with ARCH/GARCH dynamic in the variance of the factor, as presented in a companion paper. The models are based on the monthly indicator used by the National Bureau of Economic Research (NBER). The usefulness of incorporating this highly valuable credit data is measured by running the models taking both the real monthly economic data and the credit spreads or taking the hard data only. We also bridge this nowcasting exercise to an allocation strategy in which the high frequency signal of downturn is used as a weight on a cash (risk-free) allocation allowing to modulate an exposure to a risky asset. This application demonstrates the need to incorporate ASW spreads to the information sample in order to be able to follow in a timely manner coincident macroeconomic dynamics.

The paper is organized as follows. [Section 2](#) justifies the use of assets swap spreads as real-time business cycle assessors. [Section 3](#) describes the data used in the paper. [Section 4](#) covers the MS-DFMs specifications employed in this paper. [5](#) present the Gibbs sampler algorithm implemented to estimate the models. [Section 7](#) analyses the real-time weekly

---

<sup>1</sup>Among others [Fama \(1981\)](#), [Harvey \(1988\)](#), [Hamilton and Kim \(2002\)](#), [Stock and Watson \(2003\)](#), more precisely upon corporate credit spreads as in the vein of [Gilchrist et al. \(2009\)](#) and [Faust et al. \(2011\)](#)

backtests implemented. Finally Section 8 gauges the usefulness of the signals extracted through the backtest of portfolio strategies built upon the former ones.

## 2. Asset swap spreads, a rational gauge of real economy developments

Asset swaps belong to the class of over-the-counter (OTC) contracts. More specifically it is a synthetic floating-rate note which enables the investor (*asset swapper*) to exchange a fixed-coupon bond against a floating rate (SOFR/ESTER + ASW spread). The investor takes exposure to credit risk without bearing the interest movements risk related to it. As a matter of fact if the bond issuer defaults, *the asset swapper* gets the recovery value but needs to honour the swap contract without the side funding of the bond coupon -if the position is not closed at mark-to-market value. ASW spreads can be interpreted as default risk compensations and are defined as the difference between the floating rate and the SOFR/ESTER rate. They are implied from the bond yield, prices and the forward SOFR/ESTER rate as follows solving for  $S^{ASW}$  taking notations from [De Santis \(2016\)](#):

$$(100 - P) + \sum_{m=1}^M C z_{t_m} = \sum_{m=1}^M (L_{t_{m-1}, t_m} + S^{ASW}) z_{t_m} \quad m = 1, 2, \dots, M \quad (1)$$

where  $100 - P$  is the asset value to get the full price of par,  $P$  is the full market price of the bond,  $M$  the residual maturity of the bond,  $C$  the annual bond coupon,  $z_{t_m}$  the discount factor,  $L_{t_{m-1}, t_m}$  is the forward SOFR/ESTER rate between the two cash flow dates  $t_{m-1}, t_m$  and  $S^{ASW}$  the asset swap spread.

The pricing of the ASW spreads capture asynchronous and multifrequential macroeconomic data flows materialized by a continuously updated probability of default. As [De Santis \(2016\)](#) stresses it out, "*the ASW spreads are primarily driven by the credit quality of the issuer*" and are also "*less confounded by tax and various market micro-structure effects, because the bond is not sold and investment banks' business model rotate around swap contracts*". [De Santis \(2016\)](#) shows that ASW spreads are highly correlated with yield spreads, the spreads between the yield to maturity of a bond and a risk free rate of same remaining maturity. They are moreover homogeneous across countries and over time. However, during stressed periods, liquidity premia in the ASW market tend to be smaller than in the bond market, making the ASW spread less sensitive to those periods compared to yield spreads. The basis of this paper is to consider one major feature of credit risk pricing associated to the ASW spread, as highlighted by [Aussenegg et al. \(2016\)](#), namely the negative relationship between the spread and the enterprise value which in turns depends, from a macroeconomic point of view and on synthetic indices, on the business cycle phases as perceived by market participants.

## 3. Data Used

We use in our analysis for the US seven asset swap synthetic spreads splitted in grade buckets illustrated in Figure 1 as well as four coincident monthly macroeconomic variables which are displayed in Figure 2. We use for the United States the commonly data used by the NBER to date recessions constitute our information sample: industrial production

(dIP), real manufacturing and trade sales (dRS), real personal income excluding transfer payments (dPI) and non farm payroll employment (dE). Following [Camacho et al. \(2015\)](#) we decide to keep the information sample as small as possible. Shaded areas correspond to periods of recessions as defined by the NBER. Those periods correspond to the time span between the peak to the trough along the business cycle phases.

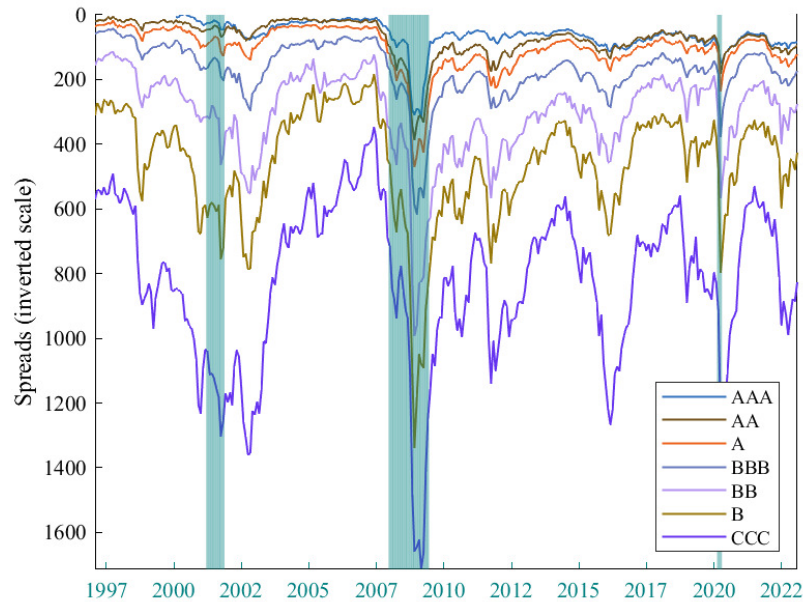


**Figure 1.** ASW spreads used

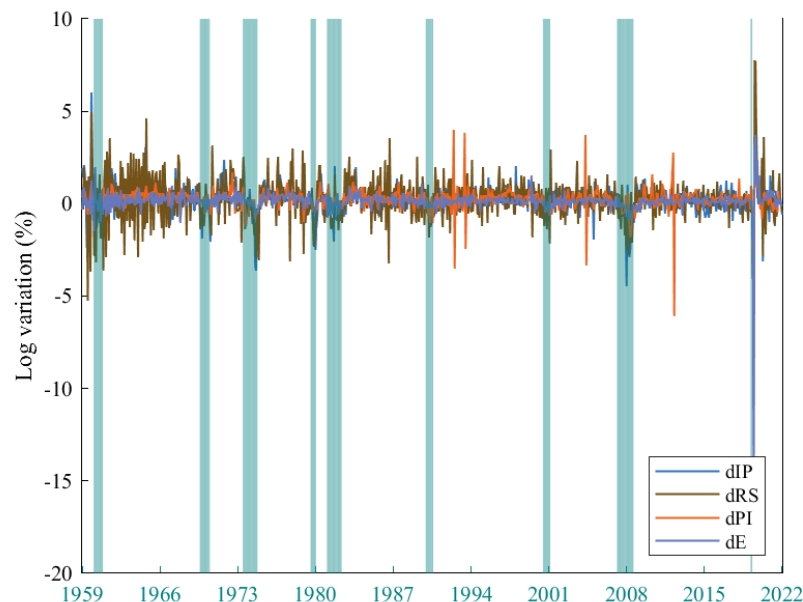


**Figure 2.** Monthly macroeconomic variables used

The four US monthly seasonally adjusted macroeconomic variables we use (what we will hereafter call hard data) stem from the FRED-MD database developed and updated

by the Federal Reserve Bank of St Louis [McCracken and Ng \(2016\)](#). Monthly vintages are available from August 1999 onwards. In the FRED-MD database, for a vintage of month M, industrial production and non farm payroll employment are displayed up until month M-1, real personal income excluding transfer payments up until month M-1 or M-2, and real manufacturing and trade sales up until month M-2 or M-3. ASW spreads are available all working days of a year and can be considered as an information directly attributable to contemporaneous assessment of the specific period.

In this paper we only focus on the contemporaneous relationships between ASW spreads and real economic activity data which are usually observed with a delay. There is at least one month lag between the first available macroeconomic data for a given monthly reference period. These data are moreover published in an asynchronous fashion. Practitioners who want to get a hint on the actual state of the economy need to wait at least one month to get new informational content on the reference period. This comes at a certain cost when one wants to develop allocation strategies based on high frequency macroeconomic signal extraction. We use the ASW spreads to "bridge" the sentiment in the credit market, measured by a broad grade-based spread contraction/widening, to the contemporaneous state of the economy in a real-time fashion. We achieve the later by taking into account the co-movement between ASW spreads and real economic variables. It is more about an analysis of the real-time assessment of the business cycle than a predictor of real activity in the sense of [Gilchrist and E.Zakrajšek \(2012\)](#)<sup>2</sup>. We therefore put aside the information from credit markets not attributable to current economic conditions. To that extent we diverge from the two-factor approach developed by [Leiva-León et al. \(2022\)](#) intending to provide a real-time gauge of a "sentiment" in credit markets, above and beyond that attributable to contemporaneous economic conditions which can cause strong asymmetric and nonlinear effects on economic activity.

## 4. Models compared

First introduced by [Diebold and Rudebusch \(1996\)](#) based on the seminal work of [Hamilton \(1989\)](#), Markov-switching dynamic factor models (MS-DFM) derived in their multivariate form by [Kim and Yoo \(1995\)](#) and afterwards used by [Chauvet \(1998\)](#) were initially applied to a set of U.S. real activity indicators at a monthly frequency with the aim of summarizing this information into a single index subject to regime changes, showing its ability to identify turning points in a timely fashion. This class of models manages indeed two characteristics of economic cycles defined by [Burns and Mitchell \(1946\)](#) : a comovement across economic series and the regime-specific nature of economic dynamics navigating through expansions and recessions. The common factor embeds the information relative to economic growth. Its dynamics defined as a Markov-chain process enable to seize the two-regime nature of the economic cycle. [Chauvet and Piger \(1998\)](#) show that Markov-switching dynamic factor models outperform alternative nonparametric methods when inferring U.S. recessions as dated by the NBER. Following [Hamilton \(1989\)](#), previous MS-DFM have assumed that the MS-constant holds for all the expansions for all recessionary episodes. We compare two competitive MS-DFM specifications using an information sample with only hard data, both real and ASW spreads to show the added value of more timely available data. [Camacho et al. \(2018\)](#) highlighted the ability of this class

---

<sup>2</sup>The authors do allow in their regression the possibility of forecasting at a zero-horizon falling into our nowcasting framework.

of model to handle asynchronous data releases, which is a key aspect of the real-time analysis we want to dig into.

The first specification used builds upon [Chauvet \(1998\)](#) where a unique Markov process drives both the constant and the variance in the state-space transition equation of the unobserved component extracted from the co-movement of the observable variables. The intuition of the business cycle, associated to the common component, being dependent on the volatility is based on the literature highlighting the usefulness of second moments to infer macroeconomic fluctuations (see [McConnell and Perez-Quiros \(2000\)](#), [Bai and Wang \(2011\)](#), and [Chauvet et al. \(2015\)](#), [Doz et al. \(2020\)](#)). We can moreover justify the use of this specification observing the [Figure 1](#) where a specific stress in the ASW market is associated to a macroeconomic vulnerability or contraction both in the United States.

$$Y_t = \Lambda F_t + u_t \quad (2)$$

$$u_{i,t} = \psi_{i,1}u_{i,t-1} + \psi_{i,2}u_{i,t-2} + e_{i,t} \quad e_{i,t} \sim \mathcal{N}(0, \sigma_{e,i}^2) \quad \text{for } j = 1 \dots n \quad (3)$$

$$F_t = \mu_{S_t} + \epsilon_t \quad \epsilon_t \sim \mathcal{N}(0, \sigma_{\epsilon, S_t}^2) \quad (4)$$

We define as  $S_t$  an independent two-state first-order Markov-Switching variable with transition probabilities given by  $p(S_t = 0 | S_{t-1} = 0) = q$  and  $p(S_t = 1 | S_{t-1} = 1) = p$ .  $S_t = 1$  corresponds to a contractionary regime whereas  $S_t = 0$  denotes a expansionary regime.  $y_t$  is the vector of  $n$  observable variables,  $F_t$  captures common fluctuations across  $Y_t$  and is composed of  $m$  components.  $u_t$  is the idiosyncratic error term which follows an autoregressive and is orthogonal to  $F_t$ .  $F_t$  follows an autoregressive process with a Markov-Switching intercept and variance. The Markov-switching intercept is defined as  $\mu_{S_t} = \mu_0(1 - S_t) + \mu_1 S_t$  and the Markov-switching variance  $\sigma_{\epsilon, S_t}^2 = \sigma_{\epsilon, 0}^2(1 - S_t) + \sigma_{\epsilon, 1}^2 S_t$ .

$$F_t = \mu_{S_t} + \epsilon_t \quad \epsilon_t \sim \mathcal{N}(0, \sigma_{\epsilon, t}^2) \quad (5)$$

The variance  $\sigma_{\epsilon, t}^2$  follows then either a ARCH(1) or a GARCH(1,1) dynamic defined in [\(6\)](#) and [\(7\)](#) :

$$\sigma_{\epsilon, t}^2 = \omega + \alpha \epsilon_{t-1}^2 \quad (6)$$

$$\sigma_{\epsilon, t}^2 = \omega + \alpha \epsilon_{t-1}^2 + \beta \sigma_{\epsilon, t-1}^2 \quad (7)$$

With  $\omega > 0$ ,  $\alpha > 0$  and  $\beta > 0$  as well as  $\alpha < 1$  or  $\alpha + \beta < 1$  to insure the positiveness and stationarity of the process  $\sigma_{\epsilon, t}^2$ .

## 5. Estimation procedure : Gibbs sampling

We define  $\theta$  the parameters vector depending on the selected specification as :

$$\theta_{MeanVar} = \{\mu_0, \mu_1, \phi, p, q, \Lambda, \Phi, \psi_{i,1}, \psi_{i,2}, \sigma_{\epsilon, 0}^2, \sigma_{\epsilon, 1}^2, \sigma_e^2\}$$

$$\theta_{MeanARCH} = \{\mu_0, \mu_1, \phi, p, q, \Lambda, \Phi, \psi_{i,1}, \psi_{i,2}, \omega, \alpha, \sigma_e^2\}$$

$$\theta_{MeanGARCH} = \{\mu_0, \mu_1, \phi, p, q, \Lambda, \Phi, \psi_{i,1}, \psi_{i,2}, \omega, \alpha, \beta, \sigma_e^2\}$$

In the following part of the paper we refer to  $X^{(T)}$  as defined by:  $X^{(T)} = \{X_1, \dots, X_T\}$ . We use the Gibbs sampling procedure proposed by [Kim and Nelson \(1998\)](#) to estimate the Markov switching state-space framework. The procedure is composed of three main blocks. The Gibbs sampler simulates draws from the joint distribution  $p(F^{(T)}, S^{(T)}, \theta | Y^{(T)})$  by sequentially drawing from the following conditional distributions :

1.  $p(F^{(T)} | Y^{(T)}, S^{(T)}, \theta)$  , following [Carter and Kohn \(1994\)](#) on the state space representation given by the observation equation (2) and the transition equation given by (4)
2.  $p(S^{(T)} | Y^{(T)}, F^{(T)}, \theta)$  , following, again, [Carter and Kohn \(1994\)](#) based on the equation (4)
3.  $p(\theta | Y^{(T)}, F^{(T)}, S^{(T)})$  given commonly used conjugate priors

The details of the state space model as well as the algorithm are described in Appendices [B](#) and [C](#).

## 6. In sample probabilities

We first estimate the models on the monthly datasets based either on the hard data sample only or on the dataset composed of both ASW spreads and hard data. The time spans from January 1959 to May 2023. The ASW spreads are available from 1997 onward. We compare the probabilities of being in recession with regards to shaded NBER dated recessions in [Figures 3](#) and [4](#).

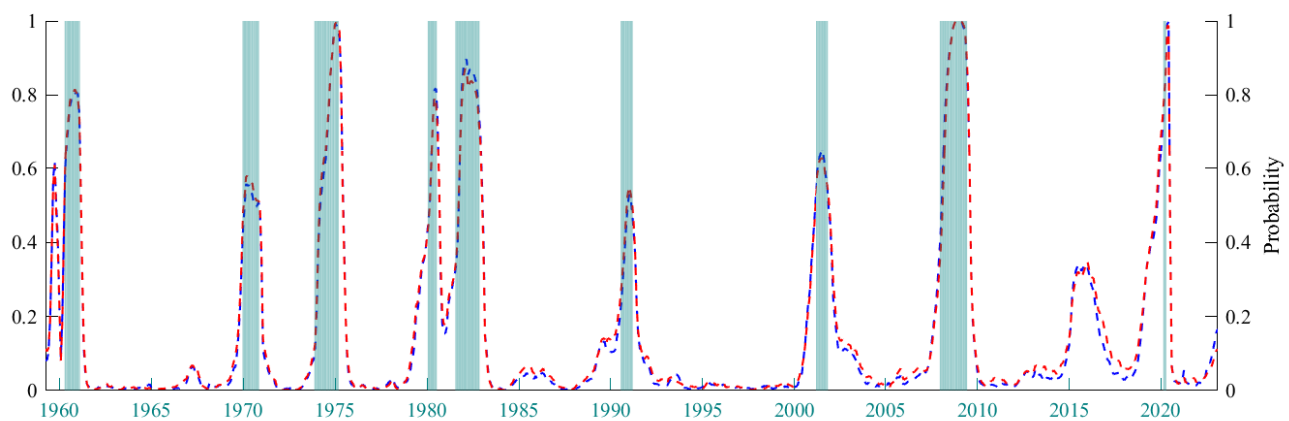


**Figure 3.** MS Mean ARCH in sample probabilities ran on US data from 1959 to 2023 on a monthly basis (blue line : hard data only, red line : hard and spread data combined)

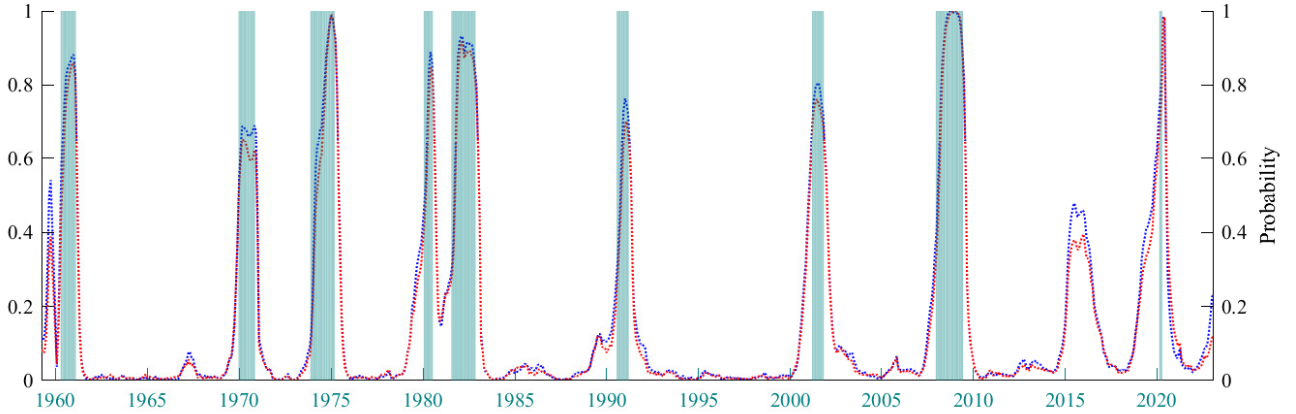


**Figure 4.** MS Mean GARCH in sample probabilities ran on US data from 1959 to 2023 on a monthly basis (blue line : hard data only, red line : hard and spread data combined)

At first sight the MS Mean GARCH specification performs better in terms of downturn identification. Adding the ASW spreads to the hard data sample does not hamper nor improve the identification. We will show in the following section that the usefulness of adding the asset swap spreads to the hard data sample arises in a real-time use of the downturn assessors.

## 7. Real-time assessments of downturns

We perform a weekly real-time assessment of the models compared on the basis of an information sample either only composed of hard data or spreads data or hard and spread data combined together. To achieve this exercise we use the rules of weekly publication of Table 1 in a given month for the data described in Section 3.

**Table 1.** Usual weekly publication schedule of US data in a given month of 5 weeks

| Month | IP | RS | PI | E |
|-------|----|----|----|---|
| w1    |    |    |    | x |
| w2    | x  |    |    | x |
| w3    | x  |    |    | x |
| w4    | x  | x  | x  | x |
| w5    | x  | x  | x  | x |

For a given month in the United States, only employment data for the reference period M-1 are available at the end of the first week. One can easily get a hint of the usefulness for a practitioner to get valuable market information up until the moment he runs his turning point nowcast. We measure the performance of adding ASW spread data to our information sample, comparing its performance to a sample composed solely by hard data using the quadratic probability score (QPS), the False Probability Score (FPS) and the Area under the Receiver Operating Characteristic curve (AUC). We show below the benefit of adding ASW spreads as business cycle real-time assessors. The main drawback

of the information sample used is the availability of the data. Indeed, asset swap spreads indices are available since 1995 in the US. However, adding this valuable information in a timely fashion due the ever-growing interactions between wall and main street dynamics shall be taken into account. The QPS is defined as follows :

$$QPS = \frac{1}{T} \sum_{t=1}^T (S_t - P(S_t = 1 | I_t))^2 \quad (8)$$

With  $S_t$  the recession dummy provided by the NBER business cycle dating committee. As the carried out backtest is implemented on a weekly basis to match the practitioner usual usage of nowcasting tools we make the hypothesis that the recession start at the first week of the month of the recession dating. This hypothesis might underestimate the ability of the ASW market to correctly track economic downturns.  $P(S_t = 1 | I_t)$  is the filtered probability inferred by the model regarding the occurrence of the regime switch to a contractionary episode given an information sample available  $I_t$ . The FPS is given by :

$$FPS = \frac{1}{T} \sum_{t=1}^T (S_t - I_{P(S_t=1|I_t)>0.5})^2 \quad (9)$$

The AUROC, the area under the Receiver Operating Characteristic (ROC) curve intends to gauge the ability of a model to discriminate between the states of a process. The ROC curve quantifies the accuracy of identification of each state as a fraction of correctly identified recessionary episodes and a fraction of missed expansionary episodes as the classification threshold  $\alpha$  varies. A performing regime identifier induces a higher ratio of correct guesses and a lower percentage of mistakes for a given  $\alpha$ . The Area Under the ROC curve is defined as the integral over the  $\alpha$  discrimination thresholds. Thus the AUROC takes values in  $[0,1]$ , AUROC = 1 being a measure for an identifier performing perfectly.

We compare the three models defined in Section 4. The backtest is ran, for comparison purposes across the information samples from 2007 to 2023. Results of the real-time exercise on US data are reported in Table 2. The weekly backtest displays the ability of spread data to accurately assess the downturns episodes in a real-time fashion when added to the usual hard data information sample. This confers a highly valuable information regarding the state in which the economy currently is. Regarding the model specifications, adding a dynamic variance to the common factor proves to be more effective in discriminating between states of the economy. The GARCH extension is the specification which performs best across the FPS, QPS and AUC performance metrics.

**Table 2.** Real-Time backtest on US data from 2007 to 2023 on a weekly basis

| US            | hard data only |      |       | hard & spreads data |             |             |
|---------------|----------------|------|-------|---------------------|-------------|-------------|
|               | FPS            | QPS  | AUROC | FPS                 | QPS         | AUROC       |
| MS Mean Var   | 0,15           | 0,14 | 0,88  | <b>0,08</b>         | <b>0,10</b> | <b>0,90</b> |
| MS Mean ARCH  | 0,11           | 0,08 | 0,90  | <b>0,09</b>         | <b>0,06</b> | <b>0,93</b> |
| MS Mean GARCH | 0,12           | 0,09 | 0,90  | <b>0,09</b>         | <b>0,06</b> | <b>0,94</b> |

Note : Bold statistics display the minimum value accross FPS and QPS statistics and maximum AUROC statistic for a given model.

Moreover, looking at the filtered probabilities in Figures 5 and 6, one can see the ability of the new information sample to catch in a very simultaneous way the downturn signals. This fact is also highlighted in Appendix D during the selected downturn episodes composed of the Great Financial Crisis and the Covid recession. The interesting pattern of the filtered probabilities from the models based on the both samples combined is their ability to capture the occurrence of the downturn signal before the models only based on the hard data sample. They also display the ability to react more quickly to the end of the downturn episode.

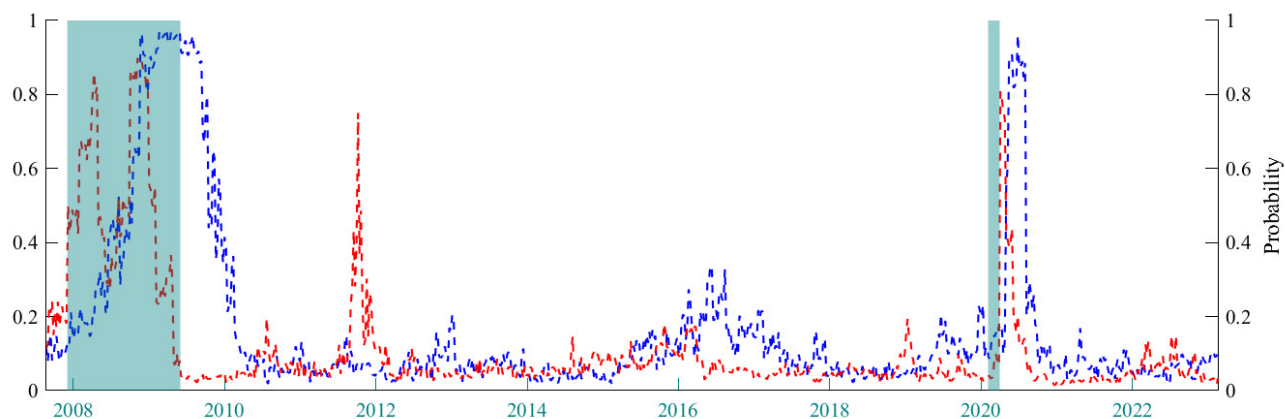


**Figure 5.** MS Mean ARCH Filtered probabilities of the Real-Time backtest run on US data from 2007 to 2023 on a weekly basis (blue line : hard data only, red line : hard and spread data combined)

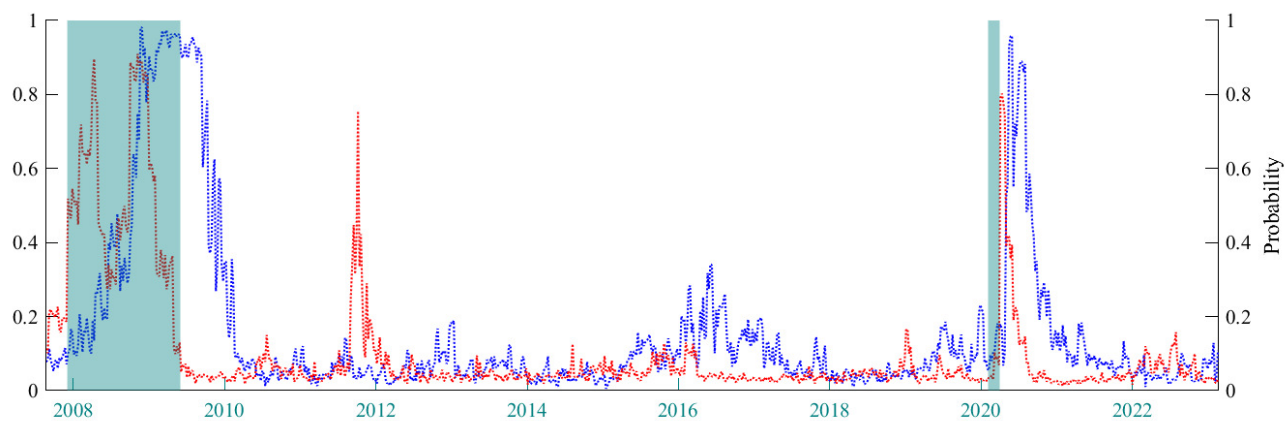


**Figure 6.** MS Mean GARCH Filtered probabilities of the Real-Time backtest run on US data from 2007 to 2023 on a weekly basis (blue line : hard data only, red line : hard and spread data combined)

We have implemented real time backtests from 2007 onwards in order to have a significative number of ASW spreads monthly observations when estimating the model on the combined dataset. In appendix E, all the out of sample filtered probabilities beginning early January 2000 are displayed. The performance metrics remain broadly unchanged. They also validate that the MS GARCH specification on an information sample composed of ASW spreads and hard data is the most effective on this longer test period.

## 8. Asset allocation strategies based on signals extracted

One of the well-known features of financial markets is to follow closely the developments of the business cycles as phenomena such as fly-to-quality reactions and forward looking valuations tend to impose a specific temporality in the market sentiment about real economy phases. A vast strand of literature has focused on the links of real business conditions and stock price variations, among others [McQueen and Roley \(1993\)](#) and more recently [Heinlein and Lepori \(2022\)](#). Markets usually react in a contemporaneous manner to the downturn, forward earnings for equity markets being revised and investors looking for more secure securities. The markets display an interesting behavior when it comes to the recovery phases. In the past major economic downturns one can observe the a rebound in the risky assets classes before the end of main street downturn. This fact is depicted in Figure 7.

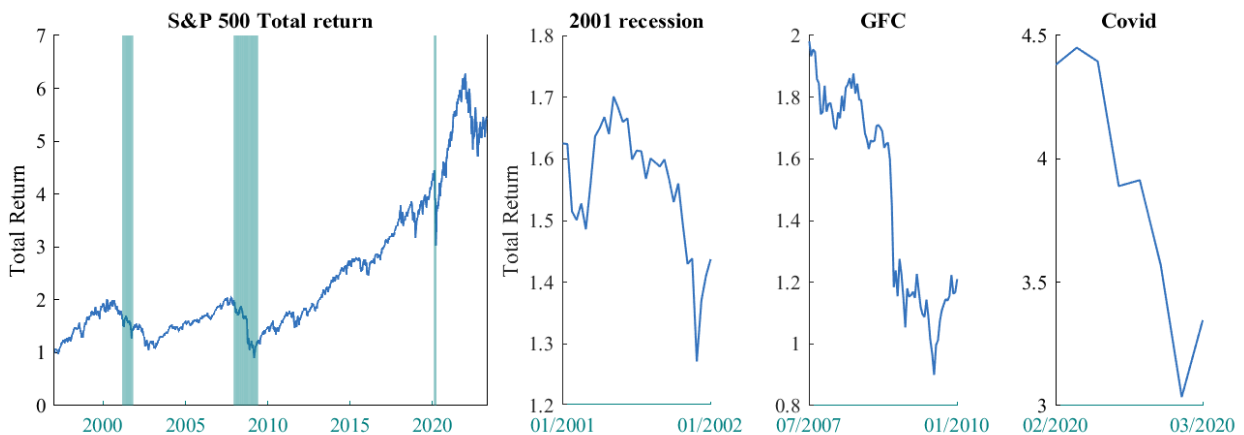


**Figure 7.** S&P 500 Total Return and selected economic downturns

We use the filtered weekly macro signals obtained in Section 7 to gauge the benefits of using asset swap spreads as real-time business cycle phase assessor in the context of portfolio management. We develop and backtest an allocation strategy based on two securities, a risky one, the equity indices S&P 500 for the US and 3M deposits rate as risk-free asset in Dollar. We define the weight of the asset *Equity* and *Cash* at a given week  $t$  as follows :

$$w_{t,Equity} = 1 - P(S_t = 1 | I_t) \quad w_{t,Cash} = P(S_t = 1 | I_t) \quad (10)$$

The bigger the probability of recession the lower the exposure to the risky asset. The underlying intuition is based on Figure 8. We show the total return of the equity indices and the cash holding from 2007 onward as well as a hypothetical strategy built upon the recession dates produced by the NBER. Whenever a recession occurs, the weight of the risky asset in the portfolio is set to 0 and the weight of cash is set to 1. This is a typical insurance-based allocation strategy where the investor discards his/her exposition to the risky asset. This strategy is considered hypothetical as the dating committee produces ex-post recession dates (determinations can take between 4 and 21 months) the practitioner does not observe in real-time. Avoiding the drawdown and being able to catch-up the recovery phase is key for market performances as highlighted by the Figure

8. We thus track the macroeconomic environment by the use of out of sample nowcast recessions signals from the three competitive models implemented on the two different types of datasets. We compare the performances of the strategies through annualised return and Sharpe ratios<sup>3</sup> we want to maximize, annualised volatility and annualised maximum drawdown we seek to minimize. The exercise is also augmented by the same descriptive statistics computed on weekly rolling windows of lengths ranging from 1 to 5 years to mitigate the entry point impact in the backtest exercise. The end of week prices used are the friday ones as the impact of the economic news releases embedded in the Employment Situation Summary produced by the BLS is fully incorporated in the prices of ASW spreads and S&P 500. The allocation rule defined in (10) defines a dynamic allocation rule which induces rebalancing of the portfolio at the end of each week. We take in our backtest exercise transaction costs of 5 basis points for the risky asset and 2 basis points for the risk-free securities. Finally, the backtest is carried out from August 2007 to February 2023.

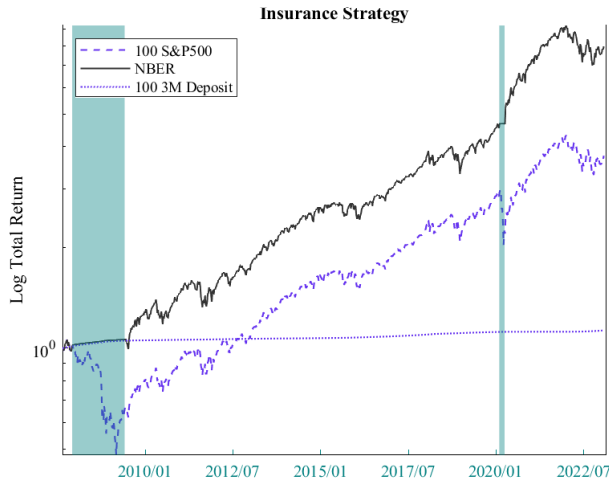


**Figure 8.** Total return of the securities used in the allocation strategy

Results of the backtest exercises are reported in Table 3 for the US. We compare the allocation strategies to two benchmarks : the hypothetical NBER categorical allocation and the constant holding of 100% of equity. The reported statistics for the US shed light on the capability of the datasets composed of both hard data and ASW spreads to perform very well in terms of risk-return allocation either on a annualised basis or on rolling windows from one to five years. One can notice that there is a clear relationship between models and datasets accurate in the turning point detection and strategies performances. Indeed, the MS Mean GARCH specification incorporating the ASW spreads datasets maximizes the accuracy metrics in discriminating the business cycle phases according to Tables 3 or 5. It is also the best performing strategy when looking at the Risk-return Sharpe ratio measures. Secondly, the strategies beat their benchmarks of holding 100% of the risky asset.

<sup>3</sup>The Sharpe ratio is defined in our case as the difference between the return of the strategy and the risk-free asset return divided by the volatility of the strategy

**Table 3.** Descriptive statistics of the strategies implemented for the US

|                       | MS Mean Var |              | MS Mean ARCH |              | MS Mean GARCH |              | Benchmark  |              |
|-----------------------|-------------|--------------|--------------|--------------|---------------|--------------|------------|--------------|
|                       | hard        | hard spreads | hard         | hard spreads | hard          | hard spreads | 100 S&P500 | NBER         |
| Annualised return     | 5,1%        | <b>7,1%</b>  | 6,2%         | <b>9,2%</b>  | 6,7%          | <b>9,4%</b>  | 8,9%       | <b>14,4%</b> |
| Annualised volatility | 12%         | 13%          | 16%          | 16%          | 15%           | 16%          | 19%        | 15%          |
| Annualised sharpe     | 0,435       | <b>0,545</b> | 0,390        | <b>0,577</b> | 0,451         | <b>0,587</b> | 0,472      | 0,982        |
| Maximum drawdown      | 24%         | 27%          | 41%          | 42%          | 34%           | 41%          | 55%        | 24%          |
| Average return 1Y     | 6,6%        | <b>8,7%</b>  | 8,5%         | <b>11,7%</b> | 8,8%          | <b>11,8%</b> | 12,0%      | <b>16,7%</b> |
| Average volatility 1Y | 10%         | 12%          | 14%          | 15%          | 13%           | 15%          | 17%        | 13%          |
| Average sharpe 1Y     | 0,592       | <b>0,692</b> | 0,549        | <b>0,746</b> | 0,605         | <b>0,757</b> | 0,671      | 1,212        |
| Maximum Drawdown 1Y   | 9%          | 10%          | 12%          | 13%          | 11%           | 13%          | 14%        | 9%           |
| Average return 2Y     | 6,9%        | <b>9,0%</b>  | 9,0%         | <b>11,8%</b> | 9,1%          | <b>11,9%</b> | 12,2%      | <b>15,7%</b> |
| Average volatility 2Y | 10%         | 12%          | 14%          | 15%          | 13%           | 15%          | 17%        | 14%          |
| Average sharpe 2Y     | 0,636       | <b>0,714</b> | 0,591        | <b>0,758</b> | 0,631         | <b>0,767</b> | 0,694      | <b>1,093</b> |
| Maximum Drawdown 2Y   | 11%         | 13%          | 16%          | 17%          | 15%           | 16%          | 18%        | 12%          |
| Average return 5Y     | 8,1%        | <b>9,4%</b>  | 10,7%        | <b>12,4%</b> | 10,6%         | <b>12,5%</b> | 13,1%      | <b>15,5%</b> |
| Average volatility 5Y | 10%         | 11%          | 14%          | 14%          | 13%           | 14%          | 16%        | 14%          |
| Average sharpe 5Y     | 0,752       | <b>0,778</b> | 0,732        | <b>0,834</b> | 0,753         | <b>0,839</b> | 0,797      | <b>1,080</b> |
| Maximum Drawdown 5Y   | 14%         | 17%          | 20%          | 21%          | 19%           | 21%          | 23%        | 16%          |

Taking into account the economic regime specification is of high interest for practitioners. We observe nonetheless the lag associated with the economic downturn detection using only macroeconomic vintaged data on a weekly basis. This fact is depicted in the Figures 5 and 6. The strategies based on spread data tend to be more reactive during contraction episodes (Great Financial Crisis and Covid for the US between 2007 and 2023). It allows for a anticipated rebalancing towards the risky asset at the very end of recessionary episode as the ASW market already prices in the exit of the downturn episode as shown by Figures 14 and 15.

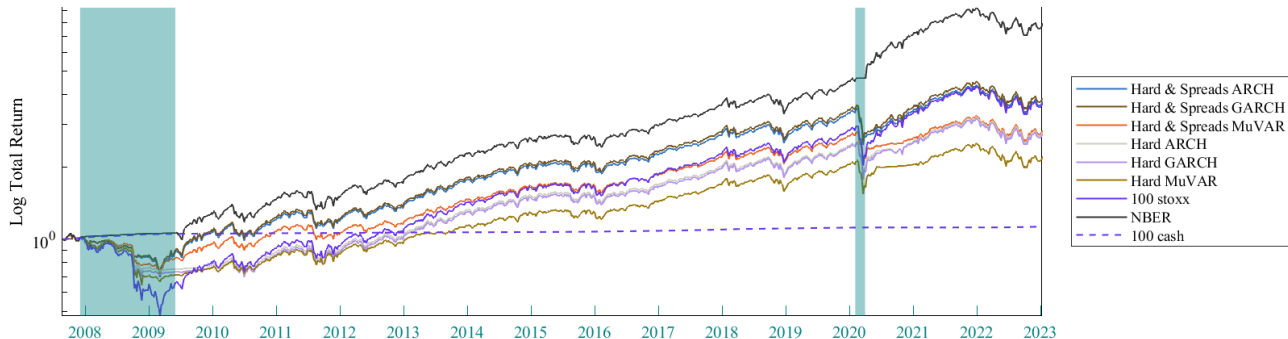


**Figure 9.** Total return of the competitive strategies based on defined information sample and models specifications

## 9. Conclusion

Tracking the business cycle phases in a real time fashion usually induces difficulties for practitioners who want to develop suitable asset allocation strategies. Macroeconomic data are indeed characterised by lags and asynchronous releases which make a real-time tracking of downturn episodes challenging. The asymmetry and heterogeneity of adverse economic phases advocate for the use of non-linear models to properly identify them. Markov Switching Dynamic factor models has shown to be a convenient class of models to handle the latter features. Nonetheless, the extraordinary episode of the Covid-19 recession and its associated variance spike, trigger the need to develop new specifications for the variance of the common component capturing the business cycle phases fluctuations.

This work builds upon the existing Markov-Switching Dynamic factor model literature to show the advantage of specifying a dynamic variance through ARCH and GARCH extensions. It also shows the usefulness for investors willing to track the US business cycles phases closely of adding market prices to the information sample usually used in the nowcasting literature. We take advantage of the co-movement between Asset Swap spreads and typical monthly indicators used in the literature to track on a weekly basis the occurrence of contractionary economic episodes.

These adverse economic episodes usually trigger ample price variations in the equity markets as risk aversion gains investors. We put forward the need for investors who want to build insurance-based strategies to use the real-time downturn probabilities as allocation rule between S&P500 and cash securities. We show that our strategy backtest outperforms the S&P500 performance.

## References

- J. H. Albert and S. Chib. Bayesian analysis of binary and polychotomous response data. *Journal of the American Statistical Association*, 88(422):669–679, 1993.
- J. Antolin-Diaz, T. Drechsel, and I. Petrella. Advances in Nowcasting Economic Activity: The Role of Heterogeneous Dynamics and Fat Tails. CEPR Discussion Papers 17800, C.E.P.R. Discussion Papers, Jan. 2023.
- W. Aussenegg, L. Goetz, and R. Jelic. European asset swap spreads and the credit crisis. *The European Journal of Finance*, 22(7):572–600, 2016.
- J. Bai and P. Wang. Conditional markov chain and its application in economic time series analysis. *Journal of Applied Econometrics*, 26(5):715–734, 2011.
- A. F. Burns and W. C. Mitchell. Measuring business cycles. *National Bureau of Economic Research*, 1946.
- M. Camacho, G. Perez-Quiros, and P. Poncela. Extracting nonlinear signals from several economic indicators. *Journal of Applied Econometrics*, 30(7):1073–1089, 2015.
- M. Camacho, G. Perez-Quiros, and P. Poncela. Markov-switching dynamic factor models in real time. *International Journal of Forecasting*, 34(4):598–611, 2018.
- C. K. Carter and R. Kohn. On gibbs sampling for state space models. *Biometrika*, 81(3):541–53, 1994.
- J. Chan and A. Grant. Modeling energy price dynamics: Garch versus stochastic volatility. *Energy Economics*, 54(C):182–189, 2016.
- J. Chan and I. Jeliaskov. Efficient simulation and integrated likelihood estimation in state space models. *International Journal of Mathematical Modelling and Numerical Optimisation*, 1:101–120, 01 2009.
- M. Chauvet. An econometric characterization of business cycle dynamics with factor structure and regime switches. *International Economic Review*, 39(4):969–996, 1998.
- M. Chauvet and J. Piger. A comparison of the real-time performance of business cycle dating methods. *Journal of Business Economic Statistics*, 26:42–49, 1998.
- M. Chauvet and Z. Senyuz. A dynamic factor model of the yield curve components as a predictor of the economy. *International Journal of Forecasting*, 32(2):324–343, 2016.
- M. Chauvet, Z. Senyuz, and E. Yoldas. What does financial volatility tell us about macroeconomic fluctuations? *Journal of Economic Dynamics and Control*, 52(C):340–360, 2015.
- R. A. De Santis. Credit spreads, economic activity and fragmentation. *European Central Bank Working Paper Series*, 1930, 2016.
- R. A. De Santis. Unobservable country bond premia and fragmentation. *Journal of International Money and Finance*, 82(C):1–25, 2018.

- F. X. Diebold and G. D. Rudebusch. Measuring business cycles: A modern perspective. *The Review of Economics and Statistics*, 78(1):67–77, 1996.
- C. Doz, L. Ferrara, and P.-A. Pionnier. Business cycle dynamics after the great recession: An extended markov-switching dynamic factor model. *PSE Working Papers*, 2020.
- E. F. Fama. Stock returns, real activity, inflation, and money. *American Economic Review*, 71(4):545–565, 1981.
- J. Faust, S. Gilchrist, J. H. Wright, and E. Zakrajšek. Credit spreads as predictors of real-time economic activity: A bayesian model-averaging approach. *National Bureau of Economic Research Working Paper*, 16725, 2011.
- S. Gilchrist and E. Zakrajšek. Credit spreads and business cycle fluctuations. *American Economic Review*, 102(4):1692–1720, 2012.
- S. Gilchrist, V. Yankov, and E. Zakrajšek. Credit market shocks and economic fluctuations: Evidence from corporate bond and stock markets. *Journal of Monetary Economics*, 56:471–493, 2009.
- J. D. Hamilton. A new approach to the economic analysis of nonstationary time series and the business cycle. *Econometrica: Journal of the Econometric Society*, page 357–384, 1989.
- J. D. Hamilton and D. H. Kim. A reexamination of the predictability of economic activity using the yield spread. *Journal of Money, Credit, and Banking*, 34(2):340–360, 2002.
- C. R. Harvey. The real term structure and consumption growth. *Journal of Financial Economics*, 22(2):305–333, 1988.
- R. Heinlein and G. M. Lepori. Do financial markets respond to macroeconomic surprises? Evidence from the UK. *Empirical Economics*, 62(5):2329–2371, 2022.
- C. Kim and C. Nelson. Business cycle turning points, a new coincident index and tests of duration dependence based on a dynamic factor model with regime switching. *The Review of Economics and Statistics*, 80(2):188–201, 1998.
- C. J. Kim and C. R. Nelson. *State space models with regime switching*. The MIT Press, Cambridge, Massachusetts, 1999.
- M.-J. Kim and J.-S. Yoo. New index of coincident indicators: A multivariate markov switching factor model approach. *Journal of Monetary Economics*, 36(3):607–630, 1995.
- D. Leiva-León, G. Pérez-Quirós, H. Sapriza, F. Vazquez-Grande, and E. Zakrajšek. Introducing the credit market sentiment index. *Richmond Fed Economic Brief*, 22(33), 2022.
- D. López-Salido, J. C. Stein, and E. Zakrajšek. Credit-market sentiment and the business cycle. *NBER Working Papers*, 21879, 2016.
- M. Marcellino, M. Porqueddu, and F. Venditti. Short-term gdp forecasting with a mixed-frequency dynamic factor model with stochastic volatility. *Journal of Business Economic Statistics*, 34(1):118–127, 2016.

- M. M. McConnell and G. Perez-Quiros. Output fluctuations in the united states: What has changed since the early 1980s? *American Economic Review*, 90(5):1464–1476, 2000.
- M. W. McCracken and S. Ng. Fred-md: A monthly database for macroeconomic research. *Journal of Business and Economic Statistics*, 34(4):574–589, 2016.
- G. McQueen and V. V. Roley. Stock prices, news, and business conditions. *Review of Financial Studies*, 6(3):683–707, 1993.
- D. O’Kane. Introduction to asset swaps. *Lehman Brothers*, 2000.
- J. Stock and M. W. Watson. *A Probability Model of the Coincident Economic Indicators*, pages 63–90. Cambridge University Press, 1991.
- J. H. Stock and M. W. Watson. Forecasting output and inflation: The role of asset. *Journal of Economic Literature*, 41(3):788–829, 2003.

# Appendices

## A. Sectoral coverage of ICE BofA Indices

| Sectors | Financial Services   | Insurance   | Automotive   |
|---------|--|---|--|
|         | Banking<br>Brokerage<br>Cons/Comm/Lease Financing<br>Investments & Misc Financial Services | Life Insurance<br>Monoline Insurance<br>Multi-Line Insurance<br>P&C | Auto Loans<br>Auto Parts & Equipment<br>Automakers |

| Sectors | Consumer Goods   | Energy   | Healthcare   |
|---------|--|--|--|
|         | Beverage<br>Food - Wholesale<br>Personal & Household Products<br>Tobacco | Energy - Exploration & Production<br>Integrated Energy<br>Oil Field Equipment & Services<br>Oil Refining & Marketing | Health Services<br>Medical Products<br>Pharmaceuticals |

| Sectors | Basic Industry  | Capital Goods  | Leisure                                 |
|---------|---|--|---|
|         | Building & Construction<br>Building Materials<br>Chemicals<br>Forestry/Paper<br>Metals/Mining Excluding Steel<br>Steel Producers/Products | Aerospace/Defense<br>Diversified Capital Goods<br>Machinery<br>Packaging | Gaming<br>Hotels<br>Recreation & Travel |

| Sectors | Media   | Real Estate                   | Retail   |
|---------|---|-------------------------------|--|
|         | Advertising<br>Cable & Satellite TV<br>Media - Diversified<br>Media Content | RealEstate Dev & Mgt<br>REITs | Food & Drug Retailers<br>Restaurants<br>Specialty Retail |

| Sectors | Services                          | Media   | Real Estate                   |
|---------|-----------------------------------|---|-------------------------------|
|         | Environmental<br>Support-Services | Advertising<br>Cable & Satellite TV<br>Media - Diversified<br>Media Content | RealEstate Dev & Mgt<br>REITs |

| Sectors | Telecommunications  | Services                          | Technology & Electronics                                      |
|---------|---|-----------------------------------|---|
|         | Telecom - Satellite<br>Telecom - Wireless<br>Telecom - Wireline Integrated & Services | Environmental<br>Support-Services | Electronics<br>Software/Services<br>Tech Hardware & Equipment |

| Sectors | Transportation   | Utilities  |
|---------|--|--|
|         | Air Transportation<br>Rail<br>Transport Infrastructure/Services<br>Trucking & Delivery | Electric-Distr/Trans<br>Electric-Generation<br>Electric-Integrated<br>Non-Electric Utilities |

## B. State space representation of the model

The model is either given by :

$$\begin{bmatrix} y_{t4,1}^{mac} \\ y_{t8,1}^{ASW} \end{bmatrix} = \begin{bmatrix} \lambda_{4,1}^{mac} \\ \lambda_{8,1}^{ASW} \end{bmatrix} F_t + \begin{bmatrix} u_{t4,1}^{mac} \\ u_{t8,1}^{ASW} \end{bmatrix} \quad u_{i,t} = \psi_{i,1}u_{i,t-1} + \psi_{i,2}u_{i,t-2} + e_t \quad e_t \sim \mathcal{N}(0, \sigma_{e,i}^2) \quad (11)$$

or

$$y_{t4,1}^{mac} = \lambda_{4,1}^{mac} F_t + u_{t4,1}^{mac} \quad u_{i,t} = \psi_{i,1}u_{i,t-1} + \psi_{i,2}u_{i,t-2} + e_t \quad e_t \sim \mathcal{N}(0, \sigma_{e,i}^2) \quad (11')$$

with index  $i$  being the line number of the information samples composed of macroeconomic hard data and asset swap spreads. The first element of  $\Lambda = [\lambda_{4,1}^{mac}, \lambda_{8,1}^{ASW}]'$  or  $\lambda_{4,1}^{mac}$  is set equal to 1 in order to achieve identification of the model. Depending on the specification of Equations (4) or (5) the factor follows either :

$$F_t = \mu_{S_t} + \epsilon_t \quad \epsilon_t \sim \mathcal{N}(0, \sigma_{\epsilon, S_t}^2) \quad (12)$$

or

$$F_t = \mu_{S_t} + \epsilon_t \quad \epsilon_t \sim \mathcal{N}(0, \sigma_{\epsilon, t}^2) \quad (12')$$

This model can be cast in state-space as follows :

$$Y_t = H Z_t + \eta_t \quad \eta_t \sim \mathcal{N}(0, R) \quad (13)$$

$$Z_t = \mu_{S_t} + \Phi Z_{t-1} + \epsilon_t \quad \epsilon_t \sim \mathcal{N}(0, Q) \quad (14)$$

with in the case of considering the hard data information sample only :

$$H = \begin{bmatrix} \lambda_1^{mac} & 1 & 0 & 0 & 0 & 0 & 0 & 0 & 0 \\ \lambda_2^{mac} & 0 & 0 & 1 & 0 & 0 & 0 & 0 & 0 \\ \lambda_3^{mac} & 0 & 0 & 0 & 0 & 1 & 0 & 0 & 0 \\ \lambda_4^{mac} & 0 & 0 & 0 & 0 & 0 & 0 & 1 & 0 \end{bmatrix} \quad Z_t = \begin{bmatrix} F_t \\ u_{1,t} \\ u_{1,t-1} \\ u_{2,t} \\ u_{2,t-1} \\ u_{3,t} \\ u_{3,t-1} \\ u_{4,t} \\ u_{4,t-1} \end{bmatrix}$$

$$\Phi = \begin{bmatrix} 0 & 0 & 0 & 0 & 0 & 0 & 0 & 0 & 0 \\ 0 & \psi_{1,1} & \psi_{1,2} & 0 & 0 & 0 & 0 & 0 & 0 \\ 0 & 1 & 0 & 0 & 0 & 0 & 0 & 0 & 0 \\ 0 & 0 & 0 & \psi_{2,1} & \psi_{2,2} & 0 & 0 & 0 & 0 \\ 0 & 0 & 0 & 1 & 0 & 0 & 0 & 0 & 0 \\ 0 & 0 & 0 & 0 & 0 & \psi_{3,1} & \psi_{3,2} & 0 & 0 \\ 0 & 0 & 0 & 0 & 0 & 1 & 0 & 0 & 0 \\ 0 & 0 & 0 & 0 & 0 & 0 & 0 & \psi_{4,1} & \psi_{4,2} \\ 0 & 0 & 0 & 0 & 0 & 0 & 0 & 1 & 0 \end{bmatrix} \quad \mu_{S_t} = \begin{bmatrix} \mu_0(1 - S_t) + \mu_1 S_t \\ 0 \\ 0 \\ 0 \\ 0 \\ 0 \\ 0 \\ 0 \\ 0 \end{bmatrix}$$

Two specifications of  $Q$  are considered :

$$Q = \begin{bmatrix} \sigma_{\epsilon, S_t}^2 & 0 & 0 & 0 & 0 & 0 & 0 & 0 & 0 \\ 0 & \sigma_{e,1}^2 & 0 & 0 & 0 & 0 & 0 & 0 & 0 \\ 0 & 0 & 0 & 0 & 0 & 0 & 0 & 0 & 0 \\ 0 & 0 & 0 & \sigma_{e,2}^2 & 0 & 0 & 0 & 0 & 0 \\ 0 & 0 & 0 & 0 & 0 & 0 & 0 & 0 & 0 \\ 0 & 0 & 0 & 0 & 0 & \sigma_{e,3}^2 & 0 & 0 & 0 \\ 0 & 0 & 0 & 0 & 0 & 0 & 0 & 0 & 0 \\ 0 & 0 & 0 & 0 & 0 & 0 & 0 & \sigma_{e,4}^2 & 0 \\ 0 & 0 & 0 & 0 & 0 & 0 & 0 & 0 & 0 \end{bmatrix} \text{ or } Q = \begin{bmatrix} \sigma_{\epsilon,t}^2 & 0 & 0 & 0 & 0 & 0 & 0 & 0 & 0 \\ 0 & \sigma_{e,1}^2 & 0 & 0 & 0 & 0 & 0 & 0 & 0 \\ 0 & 0 & 0 & 0 & 0 & 0 & 0 & 0 & 0 \\ 0 & 0 & 0 & \sigma_{e,2}^2 & 0 & 0 & 0 & 0 & 0 \\ 0 & 0 & 0 & 0 & 0 & 0 & 0 & 0 & 0 \\ 0 & 0 & 0 & 0 & 0 & \sigma_{e,3}^2 & 0 & 0 & 0 \\ 0 & 0 & 0 & 0 & 0 & 0 & 0 & 0 & 0 \\ 0 & 0 & 0 & 0 & 0 & 0 & 0 & 0 & \sigma_{e,4}^2 \\ 0 & 0 & 0 & 0 & 0 & 0 & 0 & 0 & 0 \end{bmatrix}$$

The state space modelisation composed of both hard data and ASW spread data only consists of expanding those matrices by eight lines, in order to capture a contemporaneous co-movement across macroeconomic dynamics and real-time default re-pricing.

### C. MCMC algorithm

We define  $\theta_{MeanVar} = \{\mu_0, \mu_1, \phi, p, q, \Lambda, \Phi, \psi_{i,1}, \psi_{i,2}, \sigma_{\epsilon,0}^2, \sigma_{\epsilon,1}^2, \sigma_e^2\}$  as the parameter vector. We first consider the estimation of the first specification proposed in this paper. Let's denote  $Z^{(T)} = \{Z_1, \dots, Z_T\}$  the unobserved state,  $Y^{(T)} = \{y_1, \dots, y_T\}$  the observed data and  $S^{(T)} = \{S_1, \dots, S_T\}$  the first order Markov-Chain. We describe the Gibbs sampler steps based on [Kim and Nelson \(1999\)](#). The Gibbs sampler consists of iterating between the four following steps sequentially.

#### Generation of the state vector $Z^{(T)}$

The joint distribution of  $Z^{(T)}$ , given  $Y^{(T)}$ ,  $S^{(T)}$  and  $\theta$  can be defined as :

$$p(Z^{(T)} | Y^{(T)}, S^{(T)}, \theta) = p(Z_T | Y^{(T)}, S^{(T)}, \theta) \prod_{t=1}^{T-1} p(Z_t | Y^{(t)}, S^{(t)}, \theta, Z_{t+1}) \quad (15)$$

Which boils down to generating  $Z_t$  for  $t = T, T-1, \dots, 1$  from

$$Z_T | Y^{(T)}, S^{(T)}, \theta \sim \mathcal{N}(Z_{T|T}, V_{T|T})$$

$$Z_t | Y^{(t)}, S^{(t)}, Z_{t+1}, \theta \sim \mathcal{N}(Z_{t|t, Z_{t+1}}, V_{t|t, Z_{t+1}}) \quad t = T-1, T-2, \dots, 1$$

Multi-move Gibbs sampling introduced by [Carter and Kohn \(1994\)](#) is used to generate  $p(Z^{(T)} | Y^{(T)})$  as follows.

1. We use the Kalman filter to generate  $Z_{t|t} = E(Z_t | Y^{(t)})$  and  $V_{t|t} = var(Z_t | Y^{(t)})$  for  $t = 1, \dots, T$ . The last iteration of the filter gives  $Z_{T|T}$  and  $V_{T|T}$ , which are used to generate  $Z_T$
2. For  $t = T-1, T-2, \dots, 1$ , given  $Z_{t|t}$  and  $V_{t|t}$ ,  $Z_{t+1}$  can be considered as an incremental vector of observations in the system, the distribution  $p(Z_t | Y^{(T)}, S^{(t)}, Z_{t+1})$  is then deduced from the Kalman Smoother. Considering  $Z_{t+1}$  as :  $Z_{t+1} = \mu_{S_{t+1}} + \epsilon_{t+1}$  Updating equation are then given by

$$Z_{t|t, Z_{t+1}} = Z_{t|t} + V_{t|t} \Phi \eta_t / R_t$$

$$V_{t|t, Z_{t+1}} = V_{t|t} - V_{t|t} \Phi' \Phi V_{t|t} / R_t$$

where  $\eta_t = Z_{t+1} - \mu_{S_{t+1}} - \Phi Z_{t|t}$  and  $R_t = \Phi V_{t|t} \Phi' + \sigma_{\epsilon, S_{t+1}}^2$ .

### Generation of the Markov-Chain $\mathbf{S}^{(T)}$

Once  $Z^{(T)}$  has been simulated, and given  $\theta$ ,  $S^{(T)}$  can be generated based on the following distribution:

$$\begin{aligned} p(S^{(T)} | Y^{(T)}, Z^{(T)}, \theta) &= p(S_T | Y^{(T)}, Z^{(T)}, \theta) \prod_{t=1}^{T-1} p(S_t | Y^{(t)}, Z^{(t)}, S_{t+1}, \theta) \\ &= p(S_T | Z^{(T)}, \theta) \prod_{t=1}^{T-1} p(S_t | Z^{(t)}, S_{t+1}, \theta) \end{aligned} \quad (16)$$

One can use (4) to simulate  $S^{(T)}$  as the distribution of  $S^{(T)}$  is orthogonal to  $Y^{(T)}$ , given  $Z^{(T)}$ . To generate  $S^{(T)}$  :

1. We use the [Hamilton \(1989\)](#) filter on (4) to generate  $p(S_t | Z^{(t)}, \theta)$  for  $t = 1, 2, \dots, T$  and save them. The last iteration gives  $p(S_T | Z^{(T)}, \theta)$  from which we get  $S_T$ .
2. To draw  $S_t$  given  $Z^{(T)}$  and  $S_{t+1}$ , for  $t = T - 1, T - 2, \dots, 1$  the following result is used

$$p(S_t | Z^{(t)}, S_{t+1}, \theta) = \frac{p(S_{t+1} | S_t) p(S_t | Z^{(t)}, \theta)}{p(S_{t+1} | Z^{(t)}, \theta)} \propto p(S_{t+1} | S_t) p(S_t | Z^{(t)}, \theta)$$

where  $p(S_{t+1} | S_t)$  is the transition probability and the other term is the one saved in step 1.

3. The last step consist of drawing from :

$$Pr(S_t = 1 | Z^{(t)}, S_{t+1}, \theta) = \frac{p(S_{t+1} | S_t = 1) p(S_t = 1 | Z^{(t)}, \theta)}{\sum_{j=0}^1 p(S_{t+1} | S_t = j) p(S_t = j | Z^{(t)}, \theta)}$$

By the generation of  $S_t$  from a uniform distribution (0,1). If the generated number is smaller than  $Pr(S_t = 1 | S_{t+1}, Y^{(t)}, \theta)$ ,  $S_t = 1$ , otherwise  $S_t = 0$ .

### Generation of $\theta_{\text{MeanVar}}$

#### Generation of $\lambda$

$\forall i = [2, \dots, n]$

$$\lambda_i \sim \mathcal{N}(a_i, A_i)$$

Hyperparameters are set to  $a_i = 0, A_i = 1$ . Given  $F^{(T)}$ ,  $Y^{(T)}$  and the other parameters of the mdoel,  $\lambda_i$  is generated from a modification of the (2) :

$$Y_t^* = \lambda_i F_t^* + e_{it} \quad i = 1, \dots, n$$

where  $Y_t^* = Y_t - \bar{\psi}_1 \circ Y_{t-1} - \bar{\psi}_2 \circ Y_{t-2}$  and  $F_t^* = F_t - \bar{\psi}_1 F_{t-1} + \bar{\psi}_2 F_{t-2}$ .  $\bar{\psi}_p = [\psi_{i1} \dots \psi_{ip}]'$  for  $i = 1, \dots, n$  and  $p = 1, 2$ .  $\lambda_i$  is simulated from the posterior distribution:

$$\lambda_i \sim \mathcal{N}((A_i^{-1} + \sigma_{e,i}^{-2} F^{(T)'} F^{(T)})^{-1} (A_i a_i + \sigma_{e,i}^{-2} F^{(T)'} Y^{(T)}), (A_i^{-1} + \sigma_{e,i}^{-2} F^{(T)'} F^{(T)})^{-1})$$

### Generation of $\psi, \sigma_e^2$

Commonly used priors are used for

$$\psi \sim \mathcal{N}(\pi, \Pi) \quad \pi = 0, \Pi = 1$$

$$\sigma_{e,i}^2 \sim IG(\nu_i/2, Z_i/2) \quad \nu_i/2 = 0, 1 \times T, Z_i/2 = (\nu_i/2 - 1)/10$$

Given  $W^{(T)}, Y^{(T)}$ ,  $\lambda_i$  et  $\sigma_e^2$ , the equation (2) can be rewritten :

$$y_{it} - \lambda_i F_t = u_{it}, \quad i = 1, \dots, n$$

By multiplying by  $\psi_i(L)$  on each side of the equation :

$$\psi_i(L)W_t = e_{it}, \quad i = 1, \dots, n$$

with  $\psi_i(L) = 1 - \psi_{i,1}L - \psi_{i,2}L^2$

$$W_t = \psi_{i,1}W_{t-1} + \psi_{i,2}W_{t-2} + e_{i,t}, \quad i = 1, \dots, n$$

with  $W_t = Y_t - \Lambda F_t$ .  $W^{(T)}$  is the vector of  $W_t$  and  $E_i^{(T)}$  the right hand side of the above equation, namely  $E_i^{(T)} = [e_{i,1}, \dots, e_{i,T}]'$ , for  $i = 1, \dots, n$ . The posterior distribution of  $\tilde{\psi}_i = [\psi_{i1} \dots \psi_{iP}]'$   $i = 1, \dots, n$  is given by :

$$\tilde{\psi}_i \sim \mathcal{N}((\Pi_t^{-1} + \sigma_{e,i}^{-2} E_i^{(T)'} E_i^{(T)})^{-1} (\Pi_t^{-1} \pi_i + \sigma_{e,i}^{-2} E_i^{(T)'} W^{(T)}), (\Pi_t^{-1} + \sigma_{e,i}^{-2} E_i^{(T)'} E_i^{(T)})^{-1})$$

Given the generated  $\tilde{\psi}_i$  the posterior distributions of  $\sigma_{e,i}^2$  is defined by :

$$\sigma_{e,i}^2 \sim IG\left(\frac{\nu_i + T}{2}, \frac{f_i}{2} + \frac{1}{2}(Z^{(T)} - E_i^{(T)} \tilde{\psi}_i)'(Z^{(T)} - E_i^{(T)} \tilde{\psi}_i)\right), \quad i = 1, \dots, n$$

### Generation of $\mu_{S_t}, \sigma_{\epsilon, S_t}^2$ or $\sigma_{\epsilon, t}^2$

The prior for the Markov-switching intercept is given by :

$$\begin{bmatrix} \mu_0 \\ \mu_1 \end{bmatrix} \sim \mathcal{N}(\alpha^*, A^*)$$

Hyperparameters are set equal to  $\alpha^* = \begin{bmatrix} 0 \\ 0 \end{bmatrix}$   $A^* = \begin{bmatrix} 1 & 0 \\ 0 & 1 \end{bmatrix}$

Given the generated  $\sigma_{\epsilon, S_t}^2$  or  $\sigma_{\epsilon, t}^2$  one can rewrite equation (4)

$$F_t/\sigma_{\epsilon, S_t} = \mu_1 S_t/\sigma_{\epsilon, S_t} + \mu_0(1 - S_t)/\sigma_{\epsilon, S_t} + z_t \quad z_t \sim \mathcal{N}(0, 1)$$

We denote  $G^{*(T)}$  the left-hand side of the above equation and  $Q^{*(T)}$  the right-hand side.

$\begin{bmatrix} \mu_0 \\ \mu_1 \end{bmatrix}$  can be drawn from the following posterior distribution :

$$\begin{bmatrix} \mu_0 \\ \mu_1 \end{bmatrix} \sim \mathcal{N}((A^{-1} + Q^{*(T)'} Q^{*(T)})^{-1} (A^{-1} \alpha + Q^{*(T)'} G^{*(T)}), (A^{-1} + Q^{*(T)'} Q^{*(T)})^{-1})$$

Draws verifying the condition  $\mu_0 > \mu_1$  are kept.  $\sigma_{\epsilon, S_t}^2 = \sigma_{\epsilon, 0}^2(1 - S_t) + \sigma_{\epsilon, 1}^2 S_t$  can be rewritten  $\sigma_{\epsilon, S_t}^2 = \sigma_{\epsilon, 0}^2(1 + h_1 S_t)$  where  $\sigma_{\epsilon, 1}^2 = \sigma_{\epsilon, 0}^2(1 + h_1)$ . Thus  $\sigma_{\epsilon, 0}$  can be generated given  $h_1$  by rewriting again equation (4) and deviding each side by  $\sqrt{1 + h_1 S_t}$

$$F_t/\sqrt{1 + h_1 S_t} - \mu_{S_t}/\sqrt{1 + h_1 S_t} = v_t \quad v_t \sim \mathcal{N}(0, \sigma_{\epsilon, 0}^2)$$

We define the prior :

$$\sigma_{\epsilon, 0}^2 \mid h_1, \mu_0, \mu_1 \sim IG(\kappa_0/2, \delta_0/2)$$

with hyperparameters  $\kappa_0/2 = 0, 1 \times T, \delta_0/2 = (\kappa_0/2 - 1)/10$ . We define the conjugate posterior from which we draw  $\sigma_{\epsilon, 0}^2$  :

$$\sigma_{\epsilon, 0}^2 \mid h_1, \mu_0, \mu_1, S^{(T)}, F^{(T)} \sim IG(\kappa_1/2, \delta_1/2)$$

with hyperparameters  $\kappa_1 = \kappa_0 + T, \delta_1 = \delta_0 + \sum_{t=1}^T (v_t)^2$

Once  $\sigma_{\epsilon, 0}^2$  has been generated, one can simulate  $\bar{h}_1 = 1 + h_1$  in dividing (4) by  $\sigma_{\epsilon, 0}$  :

$$F_t/\sigma_{\epsilon, 0} - \mu_{S_t}/\sigma_{\epsilon, 0} = v_t^* \quad v_t^* \sim \mathcal{N}(0, 1 + h_1 S_t)$$

We define the prior :

$$\bar{h}_1 \mid \sigma_{\epsilon, 0}, \mu_0, \mu_1 \sim IG(\kappa_2/2, \delta_2/2)$$

with hyperparameters  $\kappa_2/2 = 0, 1 \times T, \delta_2/2 = (\kappa_2/2 - 1)/10$ . We define the conjugate posterior from which we draw  $\sigma_{\epsilon, 0}^2$  :

$$\bar{h}_1 \mid \sigma_{\epsilon, 0}, \mu_0, \mu_1, S^{(T)}, F^{(T)} \sim IG(\kappa_3/2, \delta_3/2)$$

with hyperparameters  $\kappa_3 = \kappa_2 + T, \delta_3 = \delta_2 + \sum_{t=1}^T (v_t^*)^2$ .

The estimation of the ARCH and GARCH extensions follows the general steps described above. A modification has to be implemented at this step to draw the conditional variance parameter  $\sigma_{\epsilon, t}^2$ . The parameters vectors are now defined as  $\theta_{MeanARCH} = \{\mu_0, \mu_1, \phi, p, q, \Lambda, \Phi, \psi_{i,1}, \psi_{i,2}, \omega, \alpha, \sigma_e^2\}$  or  $\theta_{MeanGARCH} = \{\mu_0, \mu_1, \phi, p, q, \Lambda, \Phi, \psi_{i,1}, \psi_{i,2}, \omega, \alpha, \beta, \sigma_e^2\}$ . Instead of drawing  $\sigma_{\epsilon, S_t}$  from a posterior distribution we draw  $\gamma_{ARCH} = \{\omega, \alpha\}$  or  $\gamma_{GARCH} = \{\omega, \alpha, \beta\}$  from the following distribution  $p(\gamma \mid Z^{(T)}, S^{(T)}, \theta)$  sequentially. We use a Metropolis-Hastings such as the one used by [Chan and Grant \(2016\)](#) to sample this non-standard conditional distribution. This builds upon the precision sampler of [Chan and Jeliazkov \(2009\)](#) we add as a Metropolis-Within-Gibbs sampler step in our general Gibbs sampling estimation. As in [Chan and Grant \(2016\)](#), a Gaussian proposal centered at the mode of  $p(\gamma \mid F^{(T)}, S^{(T)}, \theta)$  is used with its covariance matrix set to be the outer product of the scores.

### Generation of $p, q$

Use of [Albert and Chib \(1993\)](#) to derive conditional distributions of  $p$  and  $q$ . Given  $S^{(T)}$  and the initial state, we denote the transition from the state  $S_{t-1} = i$  to  $S_t = j$  by  $n_{ij}$ , the log-likelihood is given by :

$$L(q, p) = q^{n_{00}}(1 - q)^{n_{01}}p^{n_{11}}(1 - p)^{n_{10}}$$

Independent beta distributions can be used as conjugate prior for each transition probability :

$$\pi(q, p) \propto q^{u_{00}}(1 - q)^{u_{01}}p^{u_{11}}(1 - p)^{u_{10}}$$

We do not put an informative prior as in [Doz et al. \(2020\)](#), instead we set  $u_{00} = u_{01} = u_{10} = u_{11} = 300$

By combining the likelihood function and the conjugate priors one can get the conditional distributions of  $[p, q]$  as the product of the independent beta distributions from which we generate  $p$  and  $q$  :

$$q \mid S^{(T)} \sim \beta(u_{00} + n_{00}, u_{01} + n_{01})$$

$$p \mid S^{(T)} \sim \beta(u_{11} + n_{11}, u_{10} + n_{10})$$

#### D. Specific downturn episodes week by week filtered probabilities and associated allocation strategies returns

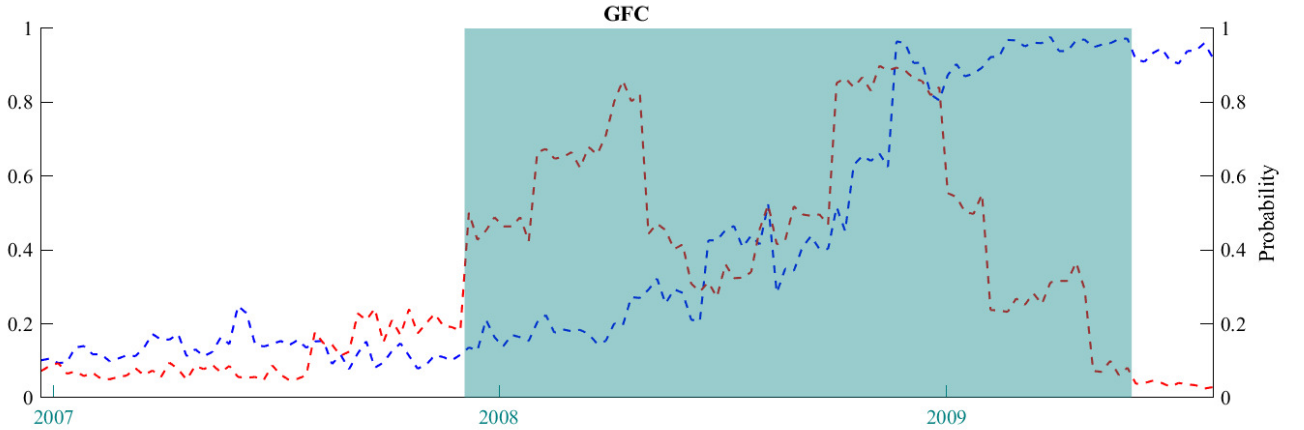


**Figure 10.** MS Mean ARCH Filtered probabilities of the Real-Time backtest during the Great Financial Crisis on a weekly basis (blue line : hard data only, red line : hard and spread data combined)

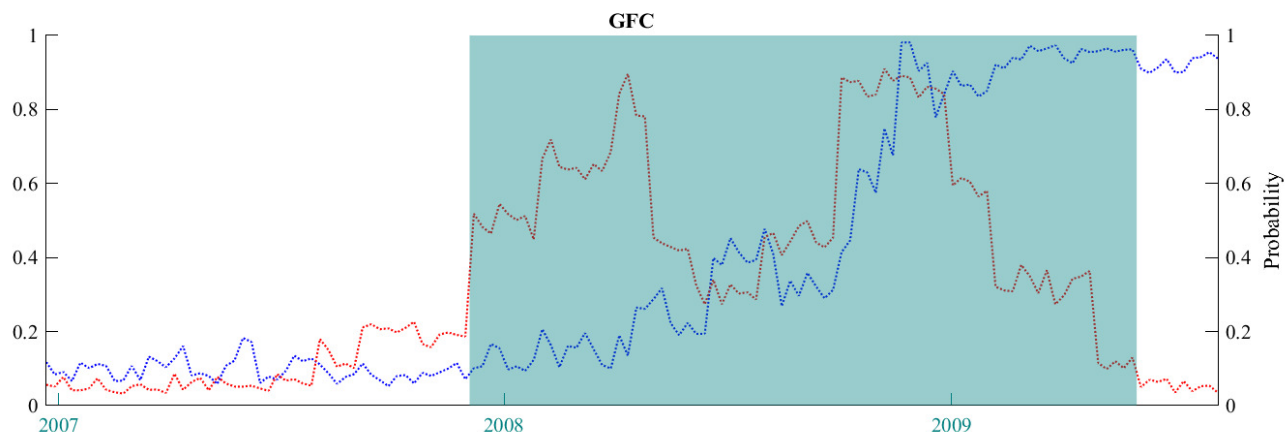


**Figure 11.** MS Mean GARCH Filtered probabilities of the Real-Time backtest during the Great Financial Crisis on a weekly basis (blue line : hard data only, red line : hard and spread data combined)

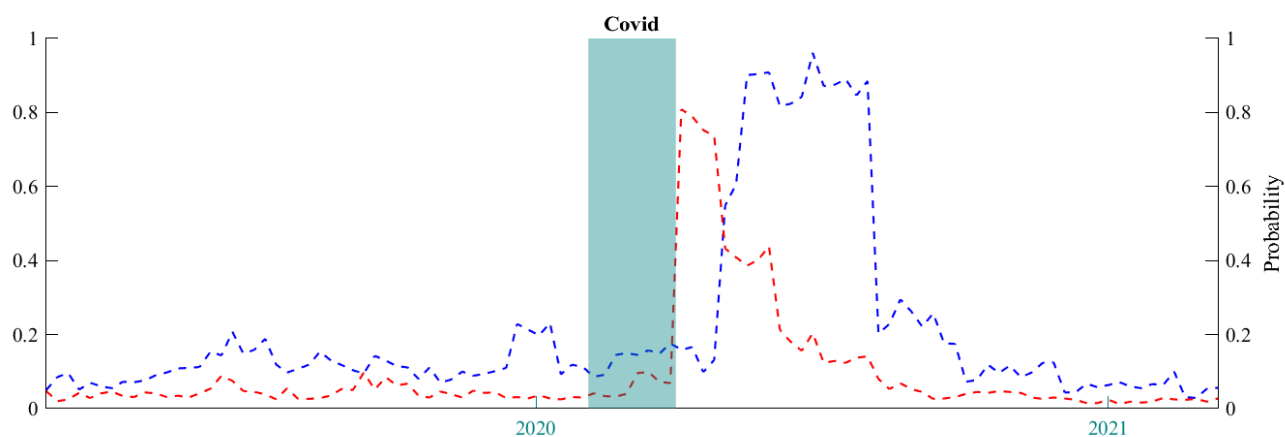


**Figure 12.** MS Mean ARCH Filtered probabilities of the Real-Time backtest during the Covid recession on a weekly basis (blue line : hard data only, red line : hard and spread data combined)

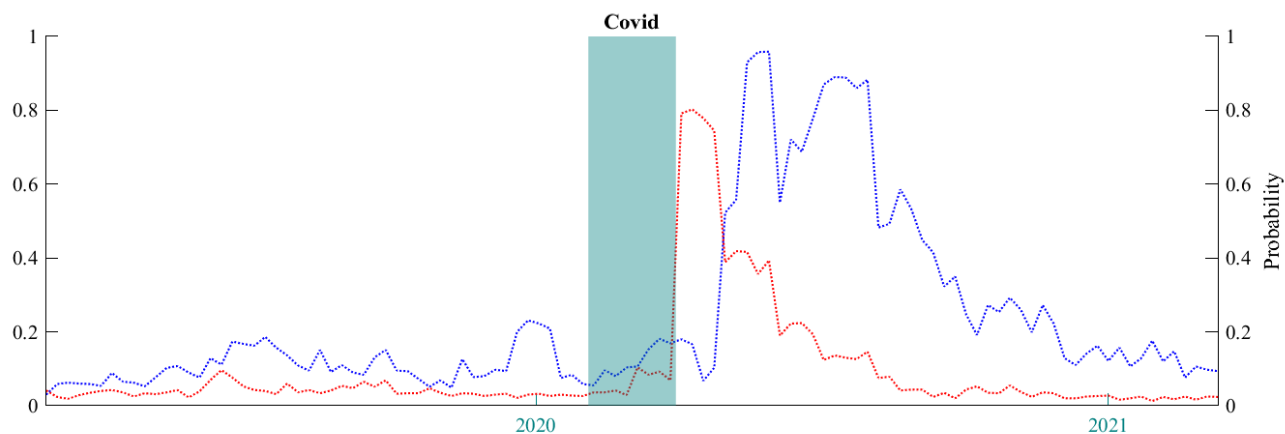


**Figure 13.** MS Mean GARCH Filtered probabilities of the Real-Time backtest during the Covid recession on a weekly basis (blue line : hard data only, red line : hard and spread data combined)

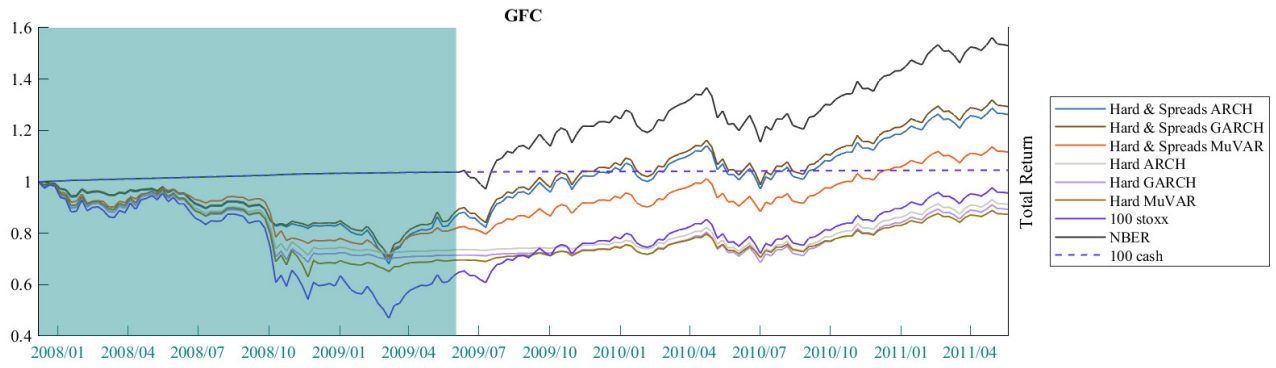


**Figure 14.** Total return of the competitive specification during the Great Financial Crisis

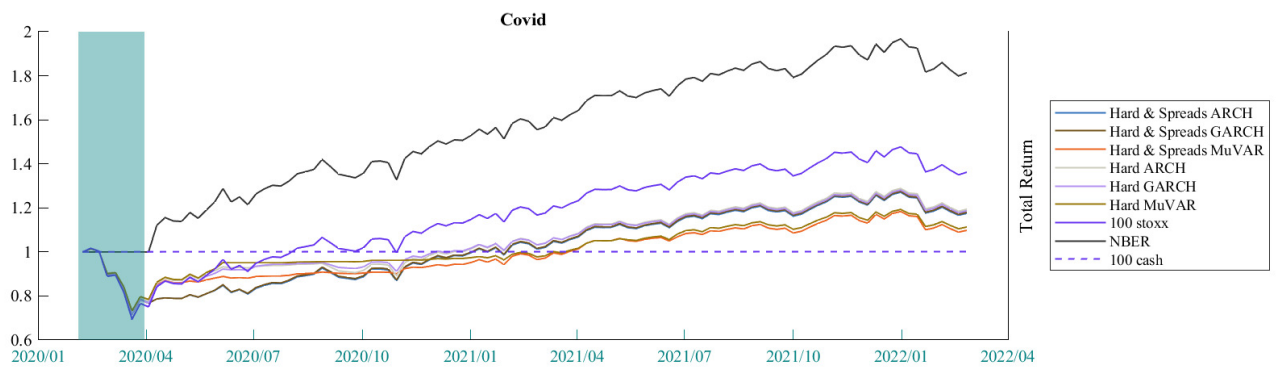


**Figure 15.** Total return of the competitive specification during the Covid Crisis

### E. Out of sample consistency check, starting backtest time date January 2000

Table 4. Real-Time backtest on US data from 2000 to 2023 on a weekly basis

| US            | hard data only |      |       | hard & spreads data |             |             |
|---------------|----------------|------|-------|---------------------|-------------|-------------|
|               | FPS            | QPS  | AUROC | FPS                 | QPS         | AUROC       |
| MS Mean Var   | 0,15           | 0,14 | 0,88  | <b>0,08</b>         | <b>0,10</b> | <b>0,90</b> |
| MS Mean ARCH  | 0,13           | 0,08 | 0,89  | <b>0,09</b>         | <b>0,06</b> | <b>0,90</b> |
| MS Mean GARCH | 0,13           | 0,09 | 0,88  | <b>0,08</b>         | <b>0,06</b> | <b>0,91</b> |

Note : Bold statistics display the minimum value accross FPS and QPS statistics and maximum AUROC statistic for a given model.

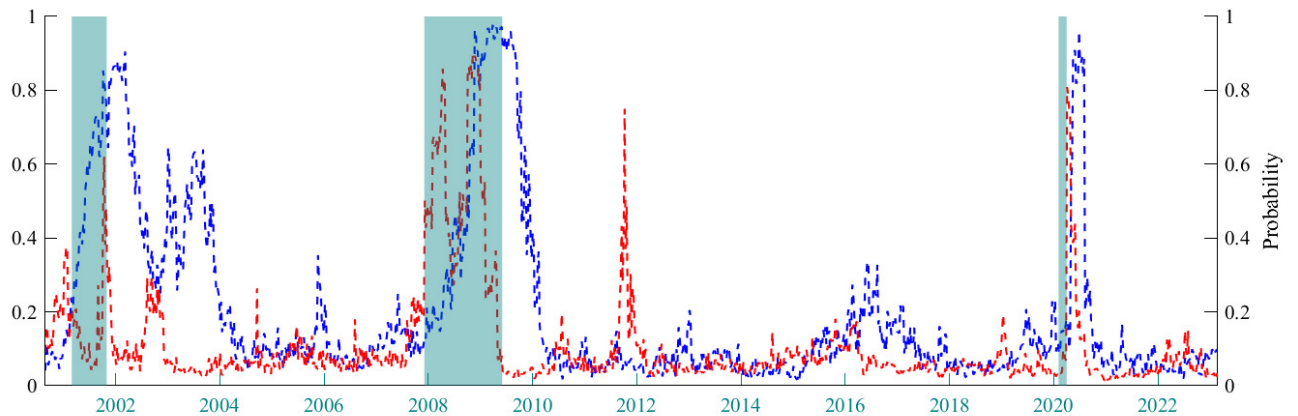


Figure 16. MS Mean ARCH Filtered probabilities of the Real-Time backtest run on US data from 2000 to 2023 on a weekly basis (blue line : hard data only, red line : hard and spread data combined)

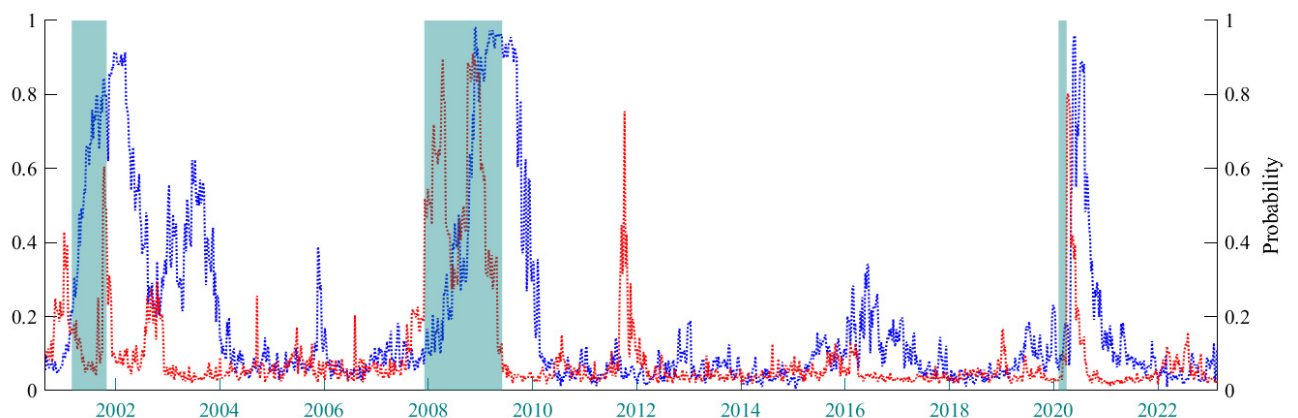
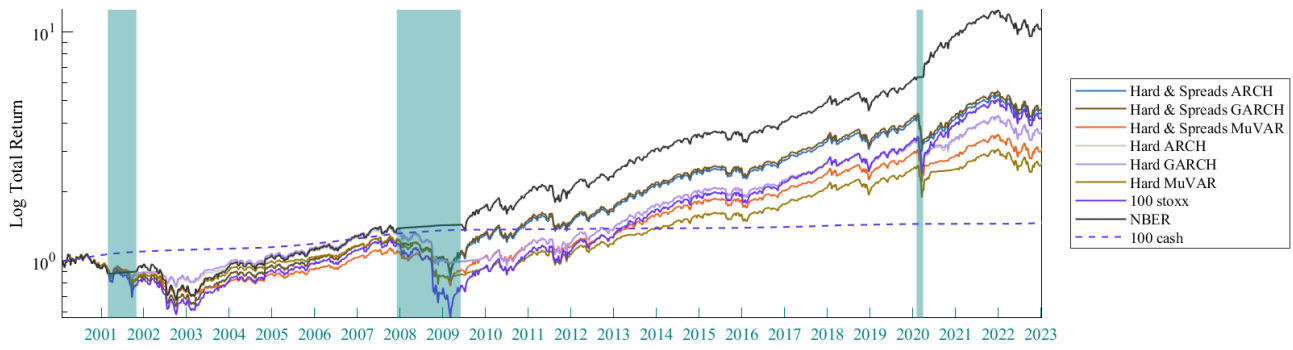


Figure 17. MS Mean GARCH Filtered probabilities of the Real-Time backtest run on US data from 2000 to 2023 on a weekly basis (blue line : hard data only, red line : hard and spread data combined)



**Figure 18.** Total return of the competitive strategies based on defined information sample and models specifications)

**Table 5.** Descriptive statistics of the strategies implemented for the US

|                       | MS Mean Var |              | MS Mean ARCH |              | MS Mean GARCH |              | Benchmark   |              |
|-----------------------|-------------|--------------|--------------|--------------|---------------|--------------|-------------|--------------|
|                       | hard        | hard spreads | hard         | hard spreads | hard          | hard spreads | 100 S&P500  | NBER         |
| Annualised return     | 4,5%        | <b>5,1%</b>  | 5,9%         | <b>6,9%</b>  | 5,9%          | <b>7,0%</b>  | 6,7%        | <b>10,9%</b> |
| Annualised volatility | 14%         | 13%          | 14%          | 15%          | 14%           | 15%          | 18%         | 15%          |
| Annualised sharpe     | 0,323       | <b>0,395</b> | 0,429        | <b>0,464</b> | 0,420         | <b>0,473</b> | 0,368       | 0,747        |
| Maximum drawdown      | 39%         | 36%          | 32%          | 41%          | 34%           | 41%          | 55%         | 38%          |
| Average return 1Y     | 5,2%        | <b>5,9%</b>  | 6,8%         | <b>8,0%</b>  | 6,8%          | <b>8,1%</b>  | <b>8,3%</b> | <b>12,2%</b> |
| Average volatility 1Y | 12%         | 12%          | 12%          | 14%          | 13%           | 14%          | 16%         | 13%          |
| Average sharpe 1Y     | 0,301       | <b>0,365</b> | 0,417        | <b>0,470</b> | 0,413         | <b>0,478</b> | 0,414       | 0,807        |
| Maximum Drawdown 1Y   | 11%         | 11%          | 11%          | 12%          | 11%           | 12%          | 14%         | 10%          |
| Average return 2Y     | 5,5%        | <b>6,1%</b>  | 7,0%         | <b>8,1%</b>  | 7,1%          | <b>8,3%</b>  | <b>8,2%</b> | <b>12,5%</b> |
| Average volatility 2Y | 12%         | 12%          | 12%          | 14%          | 13%           | 14%          | 17%         | 13%          |
| Average sharpe 2Y     | 0,317       | <b>0,388</b> | 0,436        | <b>0,481</b> | 0,429         | <b>0,492</b> | 0,399       | <b>0,819</b> |
| Maximum Drawdown 2Y   | 16%         | 15%          | 15%          | 16%          | 15%           | 16%          | 20%         | 13%          |
| Average return 5Y     | 5,3%        | <b>6,6%</b>  | 6,8%         | <b>8,8%</b>  | 6,8%          | <b>9,0%</b>  | <b>7,6%</b> | <b>11,2%</b> |
| Average volatility 5Y | 12%         | 11%          | 12%          | 13%          | 12%           | 13%          | 17%         | 13%          |
| Average sharpe 5Y     | 0,298       | <b>0,434</b> | 0,424        | <b>0,547</b> | 0,406         | <b>0,563</b> | 0,357       | <b>0,729</b> |
| Maximum Drawdown 5Y   | 23%         | 21%          | 20%          | 23%          | 21%           | 22%          | 31%         | 17%          |